The Free Surface on a Liquid between Cylinders Rotating at Different Speeds Part II

DANIEL D. JOSEPH, GORDON S. BEAVERS & ROGER L. FOSDICK

Chapter IV. The Rise of Fluid on a Rod Rotating in a Large Vat

The detailed agreement between theory and experiment which we shall display here leaves open the possibility that standard experiments on climbing can be so designed to determine accurately constants characterizing non-Newtonian fluids in slow flow. It is not possible to give a quantitative theory for the climbing observed in our experiments without accounting for the effects of surface tension.

15. Theory

In our experiments* only the inner cylinder rotates ($\lambda=0$), and the ratio of the radii of the inner and outer cylinders is essentially zero: $b=15.25$ cm, $a<0.95$ cm, $a/b<1/16$. We decided to study climbing on a rod rotating in a large stationary vat because the effect of climbing is more pronounced in the limit $a/b\to 0$ than in the limit $a/b\to 1$. When $a/b\to 1$, the basic shearing velocity varies linearly between the cylinders and, relative to the gap, the cylinders appear as moving parallel planes. If we neglect capillarity, it is easy to establish that a free surface on the sheared liquid between parallel planes will never climb. To induce normal stresses and climbing it is necessary to have large radial gradients of the circumferential shear stress. These gradients may be increased by making the radius of the rotating inner cylinder small.

In seeking a simplified theory for our experiment we replace $a/b\leqq 1/16$ with $a/b\to 0$, $b\to\infty$. Then with errors of less than one percent we take

$$B^2=a^4 \quad \text{and} \quad A\to 0,$$

and (9.21) becomes

$$h^{[2]}=\Phi^{(2)}/\rho g=-a^4/gr^2+4a^4(3\alpha_1+2\alpha_2)/\rho g r^4. \tag{15.1}$$

The first term of (15.1) would exist in a Newtonian fluid; by itself, it represents a depression in the free surface; the second, non-Newtonian term represents climbing; this second term dominates (15.1) when r is small.

* A more detailed account of these experiments by BEAVERS *et al.* is under preparation for publication in a journal of rheology.

Assuming (15.1), we note that the free surface will rise ($h>0$) when Ω is small if and only if

$$r^2<4(3\alpha_1+2\alpha_2)/\rho. \tag{15.2}$$

In our experiments $(3\alpha_1+2\alpha_2)/\rho=O(1\,\text{cm}^2)$, and in the region $r<2$ cm (approximately) the fluid will rise. It follows that when Ω is small, the fluid will not climb a rod whose radius is larger than about two centimeters. Our experiments confirm this conclusion and extend it also to large values of Ω (see Fig. 10). This is another reason why it is good to use rods of small diameter in experiments on climbing.

For small rods, (15.1) is not in good agreement with experiments because it neglects the effects of surface tension.

Two important effects of surface tension which cannot be neglected are: (i) the generation of tension forces in the surface film by displacement of the free surface and (ii) capillarity.

A convincing demonstration of the importance of the effect (i) of surface tension can be given using (12.9) and (12.10), evaluated for our experiments ($b\to\infty$). We may write (12.9) as

$$\frac{T}{r}(r h^{[2]\prime})'-\rho g h^{[2]}+\Phi^{(2)}=0, \qquad a<r<\infty, \tag{15.2a}$$

$$h^{[2]\prime}(a)=0, \qquad (h^{[2]}, h^{[2]\prime})\to(0,0) \quad \text{as} \quad r\to\infty. \tag{15.2b, c}$$

Elementary analysis of (15.2), using (15.1), shows that as $r\to\infty$

$$\rho g h^{[2]}\to\Phi^{(2)}.$$

It follows that at very large values of r, (15.1) always holds, approximately, and it is possible to neglect surface tension. In our experiments with rods smaller than 0.95 centimeters in radius the effect of surface tension on $h^{[2]}$ ceases to be sensible three to four centimeters away from the rod.

Turning next to smaller values of r, we suppose that $a\leqq r<0.95$ cm and imagine that the surface tension terms in (15.2a) are negligible. Then assuming (15.1), we find that $h^{[2]}r^4$ is nearly constant for small values of $r\geqq a$ when a is small.

Inserting $h^{[2]}r^4=\text{const.}$ into (15.2a), we find that, for our experiments (see (16.1)),

$$|T(r h^{[2]\prime})'/\rho g r h^{[2]}|=16\,T/\rho g r^2>1 \tag{15.3}$$

whenever $r<3/4$ cm. For these small values of r the surface tension term which is neglected is at least as large as the term retained. This is one reason why surface tension cannot be neglected at field points less than a few centimeters away from the axis of rotation.

The second reason for not neglecting surface tension is associated with capillarity. A wetting fluid will always climb, even when the rod does not rotate. This climbing due to wetting persists even when the rod is rotating. At the higher rates of rotation the climbing due to normal stresses increasingly dominates the climbing due to wetting, but even when the rate of rotation is not small the contribution of wetting to the rise in height of the free surface cannot be neglected (see Tables 1

Table 1. Height profiles and correction coefficients (see Fig. 5) $a=0.320$ cm, $\hat{\beta}=0.63$, $\alpha=\tan^{-1}(-\varepsilon)=-55°$, $\omega=3.8$ rev/sec

$r-a$	Total rise h as given by (16.4) $h(r; a, \hat{\beta}, \omega^2, \varepsilon)\times 10$	Rise due to wetting $h_s(r; a, \varepsilon)\times 10$ (numerical)	Correction coefficient at 2nd order $h^{[2,0]}(r; a, \hat{\beta})\times 10^4$ (numerical)	Correction coefficient at 2nd order $(h_0+h_1)\times 10^4$ (Eq. (15.20))	First approximation $h_0\times 10^4$
0	3.646	1.379	7.955	8.093	8.103
0.1	2.470	0.629	6.459	6.600	6.822
0.2	1.584	0.328	4.408	4.723	5.252
0.3	0.989	0.176	2.852	3.328	4.080
0.4	0.612	0.096	1.808	2.365	3.243
0.5	0.377	0.053	1.136	1.701	2.636
0.6	0.233	0.030	0.712	1.235	2.186
0.7	0.144	0.017	0.460	0.902	1.844
0.8	0.088	0.009	0.279	0.162	0.942
0.9	0.055	0.005	0.174	−0.040	0.580
1.0	0.034	0.003	0.108	−0.104	0.397

Table 2. Height profiles and correction coefficients (see Fig. 6) $a=0.160$ cm, $\hat{\beta}=0.63$, $\alpha=\tan^{-1}(-\varepsilon)=-46°$, $\omega=5$ rev/sec

$r-a$	Total rise h as given by (16.4) $h(r; a, \hat{\beta}, \omega^2, \varepsilon)\times 10$	Rise due to wetting $h_s(r; a, \varepsilon)\times 10$ (numerical)	Correction coefficient at 2nd order $h^{[2,0]}(r; a, \hat{\beta})\times 10^4$ (numerical)	Correction coefficient at 2nd order $(h_0+h_1)\times 10^4$ (Eq. (15.20))	First approximation $h_0\times 10^4$
0	3.196	0.982	4.486	4.765	4.958
0.1	2.003	0.428	3.192	3.586	3.967
0.2	1.148	0.215	1.890	2.504	3.099
0.3	0.651	0.125	1.092	1.827	2.539
0.4	0.371	0.068	0.630	1.388	2.156
0.5	0.213	0.032	0.364	1.087	1.879
0.6	0.123	0.018	0.212	0.869	1.668
0.7	0.072	0.010	0.125	0.706	1.503
0.8	0.042	0.006	0.073	0.284	1.021
0.9	0.025	0.004	0.044	0.152	0.783
1.0	0.015	0.002	0.026	0.030	0.649

and 2). Our computations suggest that the capillarity component of the total rise is not negligible in any of the steady configurations exhibited in the photographs of Section 16.

Of the two effects of surface tension, capillarity, though not negligible, is the less important. First, as we have mentioned, the climbing due to wetting is generally less important than climbing due to normal stresses when the angular velocity is not small. Secondly, we saw in Section 14 that the capillarity effects are expected to be confined to a narrow boundary layer of thickness $O(T/\rho g)^{\frac{1}{2}}$ where $(T/\rho g)^{\frac{1}{2}}=1/5.32$ cm in our experiment.

To study the two effects of surface tension, we turn next to the two-parameter expansion procedure which was mentioned but not developed at the end of Section 12.

We are now considering the problem (2.4) set on the domain $-\infty < z \leqq h$, $a \leqq r < \infty$ and modified so that $(\boldsymbol{u}, S, h)$ and the derivatives of

$$(\boldsymbol{u}, S, h) \to 0 \quad \text{as} \quad r \to \infty. \tag{15.4}$$

The condition $h(r) \to 0$ replaces the zero mean condition (2.1e) and fixes the origin of the coordinate z. At $r = a$ we prescribe the contact angle condition in the form

$$h'(a) = \tan\alpha = -\varepsilon. \tag{15.5}$$

We seek the solution of problem (2.4), modified for the infinite domain, as a double Taylor series

$$\begin{Bmatrix} \boldsymbol{u} \\ \Phi \\ h \end{Bmatrix} = \sum_{n=0}^{\infty} \sum_{l=0}^{\infty} \frac{\Omega^n}{n!} \frac{\varepsilon^l}{l!} \begin{Bmatrix} \boldsymbol{u}^{[n,l]} \\ \Phi^{[n,l]} \\ h^{[n,l]} \end{Bmatrix}, \tag{15.6a, b, c}$$

where

$$\boldsymbol{u}^{[n,l]} = \partial^{n+l} \boldsymbol{u}(r, z(\Omega, \varepsilon); \Omega, \varepsilon) / \partial\Omega^n \partial\varepsilon^l |_{\varepsilon=\Omega=0}$$

with similar representations for $\Phi^{[n,l]}$ and $h^{[n,l]}$. The angular velocity Ω and the contact angle $\tan^{-1}(-\varepsilon)$ are both domain parameters. The shape of the free surface varies when these parameters are varied. As in (4.1) we may define a mapping

$$z(\Omega, \varepsilon) = \phi(r_0, z_0; \Omega, \varepsilon), \tag{15.7}$$

where

$$z_0 = \phi(r_0, z_0; 0, 0) \tag{15.8}$$

and

$$h(r; \Omega, \varepsilon) = \phi(r_0, 0; \Omega, \varepsilon). \tag{15.9}$$

In forming the derivatives $[n, l]$ one must remember that the coordinate z depends on ε and Ω. For example,

$$\boldsymbol{u}^{[1,0]} = \boldsymbol{u}^{(1,0)} + \phi^{[1,0]} \partial_z \boldsymbol{u}^{(0,0)},$$

and

$$\boldsymbol{u}^{[1,1]} = \boldsymbol{u}^{(1,1)} + \phi^{[0,1]} \partial_z \boldsymbol{u}^{(1,0)} + \phi^{[1,0]} \partial_z \boldsymbol{u}^{(0,1)} + \phi^{[1,0]} \phi^{[0,1]} \partial_{zz}^2 \boldsymbol{u}^{(0,0)},$$

where

$$\boldsymbol{u}^{(n,l)} = \partial^{n+l} \boldsymbol{u}(r, \phi^{[0,0]}; \Omega, \varepsilon) / \partial\Omega^n \partial\varepsilon^l |_{\varepsilon=\Omega=0}$$

and

$$h^{[n,l]} = \phi^{[n,l]}(r_0, 0; 0, 0).$$

Returning now to (15.6), we note that the series of terms with superscripts $[n, 0]$ give the solution of the problem with neutral wetting which was considered in Section 12. The series of terms with superscripts $[0, l]$ give the solution of the problem of climbing due to wetting when there is no rotation.

Interest in climbing centers around the correction coefficients $h^{[n,l]}$ for the height h of the free surface. When there is no motion and when $\varepsilon = 0$, we have a flat surface and, of course, $h^{[0,0]} = 0$. Symmetry of the shape of the surface with

respect to changes of sign in Ω implies that

$$h^{[2n+1,\,l]}=0 \tag{15.10}$$

for all non-negative integers n and l. A different symmetry restriction applies when $\Omega=0$. When $\Omega=0$, the basic problem (2.4) governs the static rise of the fluid on a rod due to wetting:

$$\{r h_s'/(1+h_s'^2)^{\frac{1}{2}}\}' - r S h_s = 0 \qquad S=\rho g/T, \tag{15.11a}$$

and

$$h_s'(a)=-\varepsilon, \qquad (h_s, h_s')\to(0,0) \quad \text{as} \quad r\to\infty. \tag{15.11b, c}$$

It is easy to establish that the solution of (15.11) is in the form $h_s=\varepsilon H(r;\varepsilon^2)$. Therefore $h_s(r,\varepsilon)$ is an odd function of ε and $h^{[0,\,2l]}=0$.

Summarizing, we have shown that the series (15.6c) may be written as

$$h(r;\Omega,\varepsilon)=h_s(r;\varepsilon)+h^{[2,\,0]}(r)\,\Omega^2/2+\cdots \tag{15.12}$$

where the leading terms of higher order are

$$h^{[2,\,1]}(r)\,\varepsilon\Omega^2/2+h^{[4,\,0]}\Omega^4/4!+\cdots. \tag{15.13}$$

All of the higher-order terms of (15.12) involve the computation of secondary motions from difficult boundary-value problems.

In the remainder of this paper we shall assume that

$$h(r;\Omega,\varepsilon)\sim h_s(r;\varepsilon)+h^{[2,\,0]}\Omega^2/2 \tag{15.14}$$

is a good approximation for the height of the free surface when Ω is small.* The fact that $\varepsilon=O(1)$ in our experiments means that (15.14) is equivalent to an assumption that the correction coefficients $h^{[2,m]}$, $m=1,2\ldots$, are all "small". Our experiments do show that $dh/d\Omega^2$ does not change with ε when Ω is small (see (iv) of Section 16), but the actual numerical calculation of these functions of the secondary motion has not yet been carried out.**

* We mean to say that a characteristic dimensionless parameter is small. This dimensionless parameter can be written as a modified Froude number $\Omega^2 l/g$, where l is a characteristic length depending on the apparatus and the fluid. Though this length is not uniquely given and in any case must depend on unknown characterizing constants for the non-Newtonian fluid, we may guess that it is $O(h^{[2,0]}(a)\,g)^{\frac{1}{2}}$ (*cf.* (15.12)). For small values of a we find, using (15.22), that

$$g\,h^{[2,0]}(a)\approx a\sqrt{\frac{g}{\rho T}}\,(3\alpha_1+2\alpha_2)\approx 4a\ \text{cm}^2 \qquad \text{(in our experiment)}.$$

Assuming that $l=2a^{\frac{1}{2}}$, we may write the condition $\Omega^2 l/g<1$ as $\omega<(980/8a^{\frac{1}{2}}\pi^2)^{\frac{1}{2}}$ revolutions per second. This estimate is not inconsistent with the observations shown in Figs. 1 and 2. These figures show that the variation of the height is very nearly linear when $\omega^2<12/a^{\frac{1}{2}}$.

** The computation of the leading terms of (15.13) is not to be regarded as a mere correction of second-order results obtained earlier in this paper. In perturbation theories for nonlinear problems interest usually focuses on the first nonlinear corrections. Only one part of the first nonlinear correction has been computed in this paper; the second part involves numerical computation of the leading terms of (15.13). The secondary motions make their first appearance at orders $\varepsilon\Omega^2$ and Ω^4; if we are lucky, the computation of these corrections will bring theory and experiment into good agreement not only for small values of Ω but also for the larger values of Ω in the nonlinear range of the experimental height curves shown in Figs. 1 and 2.

To compute the rise of the free surface from (15.14) we must obtain the functions $h_s(r;\varepsilon)$ and $h^{[2,0]}(r)$. The static rise $h_s(r;\varepsilon)$ due to wetting is easily obtained by numerical integration.* The correction coefficient $h^{[2,0]}=a^4H$ is found as a solution of the following boundary-value problem:

$$\frac{1}{r}(rH')'-SH=-\Phi^{(2)}/Ta^4=\{\rho/r^2-4(3\alpha_1+2\alpha_2)/r^4\}/T$$

where

$$H'(a)=0, \quad (H,H')\to(0,0) \quad \text{as} \quad r\to\infty. \tag{15.15a, b, c}$$

To analyze the problem (15.15a, b, c), we combine a direct numerical analysis with an approximate solution. The approximate solution is very important in revealing the dependence of the solution on the parameters; this dependence and the one observed in the experiments agree well.

To derive a simple approximate solution of (15.15), we first rewrite (15.15a) as

$$\hat{\mathscr{L}}H=\hat{\mathscr{M}}H+f, \tag{15.15d}$$

where

$$\hat{\mathscr{L}}\circ=r\{r(\circ)'\}'-\lambda^2(\circ), \qquad \lambda^2\equiv a^2S$$

$$\hat{\mathscr{M}}\circ=(r-a^2/r)\{r(\circ)'\}'$$

$$f=\gamma/r^2-\delta/r^4$$

$$\gamma=\rho a^2/T$$

and

$$\delta=4a^2(3\alpha_1+2\alpha_2)/T.$$

We shall solve (15.15d, b, c) by successive approximations. Thus

$$H=H_0+H_1+H_2+\cdots,$$

$$\hat{\mathscr{L}}H_0=f, \tag{15.16}$$

$$\hat{\mathscr{L}}H_{n+1}=\hat{\mathscr{M}}H_n \quad (n=0,1,2),$$

where each of the approximating functions H_n satisfies the boundary conditions (15.15b, c). In forming these solutions we make repeated use of the identity

$$\hat{\mathscr{L}}(r^{-\beta})=(\beta^2-\lambda^2)r^{-\beta}. \tag{15.17}$$

We find that

$$H_0(r)=\frac{\delta}{16-\lambda^2}\left\{\frac{4a^{\lambda-4}}{\lambda r^\lambda}-\frac{1}{r^4}\right\}+\frac{\gamma}{4-\lambda^2}\left\{\frac{1}{r^2}-\frac{2a^{\lambda-2}}{\lambda r^\lambda}\right\} \tag{15.18}$$

and

$$H_1(r)=\sum_{i=1}^{5}g_i(r), \tag{15.19}$$

* When ε is small, we may linearize (15.11). Then

$$h_s(r;\varepsilon)=\varepsilon K_0(rS^{\frac{1}{2}})/S^{\frac{1}{2}}K_1(aS^{\frac{1}{2}}),$$

where K_0 and K_1 are modified Bessel functions. The error which results from using this expression is less than 10% when

$$-30^\circ<\alpha=\tan^{-1}(-\varepsilon)<30^\circ$$

where

$$g_1 = \frac{4c_1}{4-\lambda^2}\left\{\frac{1}{r^2} - \frac{2a^{\lambda-2}}{\lambda r^\lambda}\right\},$$

$$g_2 = \frac{16c_2 - 4a^2c_1}{16-\lambda^2}\left\{\frac{1}{r^4} - \frac{4a^{\lambda-4}}{\lambda r^\lambda}\right\},$$

$$g_3 = -\frac{16a^2c_2}{36-\lambda^2}\left\{\frac{1}{r^6} - \frac{6a^{\lambda-6}}{\lambda r^\lambda}\right\},$$

$$g_4 = -\frac{\lambda c_3}{2} r^{-\lambda}\{\ln r/a + 1/\lambda\},$$

$$g_5 = -\frac{\lambda^2 a^2 c_3}{4(\lambda+1)r^\lambda}\left\{\frac{1}{r^2} - \frac{\lambda+2}{\lambda a^2}\right\},$$

$$c_1 = \frac{\gamma}{4-\lambda^2},$$

$$c_2 = -\frac{\delta}{16-\lambda^2},$$

and

$$c_3 = -4a^{\lambda-4}c_2/\lambda - 2a^{\lambda-2}c_1/\lambda.$$

The expressions (15.18) and (15.19) take on an especially simple form when $r=a$. Recalling that

$$h^{[2,0]} = a^4 H = a^4(H_0 + H_1 + \cdots) = h_0 + h_1 + \cdots, \tag{15.20}$$

we find that

$$h_0(a) = \frac{a}{T\sqrt{S}}\left\{\frac{4(3\alpha_1+2\alpha_2)}{4+\lambda} - \frac{\rho a^2}{2+\lambda}\right\}$$

and

$$h_1(a) = \frac{a^2}{T(\lambda+1)(\lambda+4)}\left\{\frac{8(3\alpha_1+2\alpha_2)(\lambda-2)}{\lambda(\lambda+4)(\lambda+6)} - \frac{\rho a^2}{(\lambda+2)^2}\right\}.$$

The approximation we have used is designed to give good results near $r=a$, where the climbing is greatest. At $r=a$ the correction operator $\hat{\mathscr{H}}=0$. In Tables 1 and 2 we have compared the approximate solution (15.20) for $h^{[2,0]}=h^{[2]}$ with values computed by numerical integration of (15.2); with an error smaller than those inherent in our experiments we may take $h^{[2,0]}(a)=h_0(a)$.

In summary, when Ω is small and when we assume (15.14), we find that

$$h(r;\Omega,\varepsilon) \sim h_s(r;\varepsilon) + \left\{\frac{\delta}{16-\lambda^2}\left[\frac{4a^\lambda}{\lambda r^\lambda} - \frac{a^4}{r^4}\right] + \frac{\gamma a^2}{4-\lambda^2}\left[\frac{a}{r^2} - \frac{2a^\lambda}{\lambda r^\lambda}\right]\right\}\frac{\Omega^2}{2} \tag{15.21}$$

and

$$h(a;\Omega,\varepsilon) \sim h_s(a,\varepsilon) + \frac{a}{T\sqrt{S}}\left[\frac{4(3\alpha_1+2\alpha_2)}{4+\lambda} - \frac{\rho a^2}{2+\lambda}\right]\frac{\Omega^2}{2}. \tag{15.22}$$

The difference between (15.1), which neglects the effect of surface tension, and (15.21), which includes this effect, is striking. For example, according to (15.1), $dh/d\Omega^2|_{r=a}$ is independent of a when a is small, but according to (15.22) this slope increases linearly with a.

16. Experiments

The experimental apparatus consisted essentially of a rod of uniform diameter rotating at constant angular velocity in a vat filled with STP motor oil additive.* The diameter of the vat was 30.5 cm, and its depth was 7.7 cm. Eight different rods were used, five of which were of aluminum with radii of 0.160, 0.320, 0.635, 0.945 and 1.905 cm, and the other three were teflon-coated, with radii of 0.160, 0.320 and 0.635 cm. The vat was completely filled with STP, and the free surface

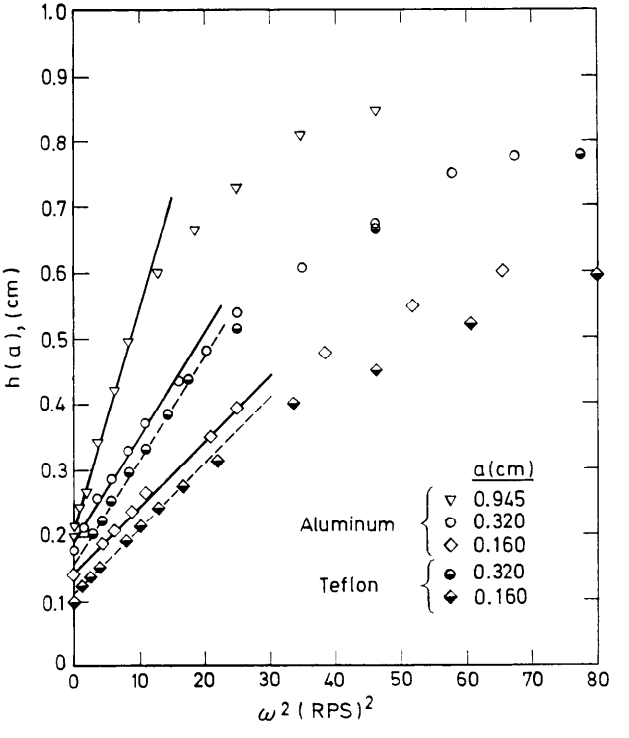

Fig. 1. The rise at $r=a$ versus the square of the angular velocity. Average contact angles: teflon, 38°; aluminum, 50°.

* Consumer Reports (**36**, 422–423, 1971) asserts that STP motor oil additive consists mainly of a polyisobutylene polymer dissolved in petroleum oil. Such a polymer-oil solution is called a viscosity index improver. When mixed with engine oil this improver helps the oil to retain its normal "thickness" despite large temperature changes. Consumer Reports disputes the claim that STP additive has a beneficial effect on the operation of automobiles, and suggests that STP does very little except to make the oil thicker than the label grade specifies. Our experiments suggest that the viscosity index measurements tell only part of the STP story; after all, such measurements cannot indicate that STP climbs up rotating rods.

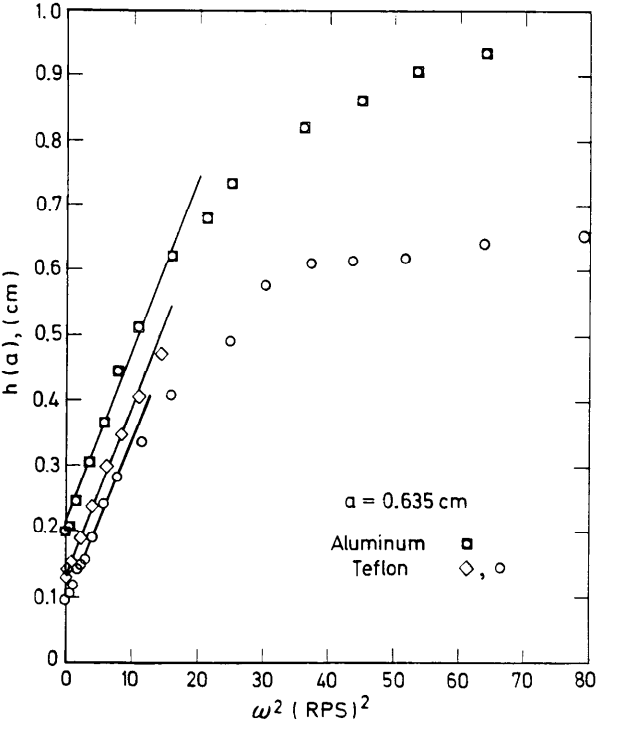

Fig. 2. The rise at $r=a$ versus the square of the angular velocity for rods with $a=0.635$ cm. Average contact angles: teflon, 38°; aluminum, 50°.

of the climbing bubble of fluid was photographed at grazing incidence across the surface of the fluid in the vat. For most of the experiments close-up Polaroid slides were produced directly, and these were then projected to give very enlarged surface profiles, which could be measured with accuracy. An accurate measurement of the angular velocity was obtained using a light source, a photomultiplier tube, and an electronic counter. For each rod, surface profiles were recorded for various values of the angular velocity up to the value at which the bubble configuration became unstable.*

The experimental data are summarized in the photographs and graphs of Figs. 1 through 10.** The photographs presented in the figures are representative of the flow configurations which were observed.

A brief survey of our observations as we increased the value of the angular velocity ω will now be given. When $\omega=0$ there is some climbing due to wetting. This climbing is very adequately described by the classical theory if the prescribed contact angle is taken at the observed values. For small values of ω the rise of the free surface at $r=a$ is proportional to ω^2; the observed values of $h(a; \omega^2, \varepsilon)$ which are shown in Figs. 1 and 2 lie on a straight line at small values of ω^2.

* A more detailed report of the experiments, including a description of the apparatus and the measuring techniques employed, will be prepared for future publication in a rheology journal.

** The dark rods in Figs. 3 through 10 are aluminum, and the white rods are teflon-coated.

a

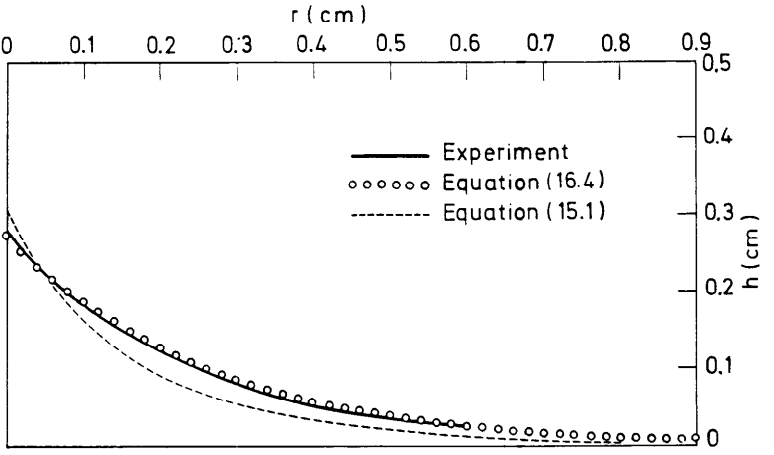

b

Fig. 3. a) The free surface on STP motor oil additive near a rod of radius $a=0.635$ cm rotating at $\omega=2.5$ rev/sec in a large vat; $\omega^4<144/a$, $\alpha=50°$.
b) Comparison of experimental and theoretical profiles ($\hat{\beta}=0.63$).

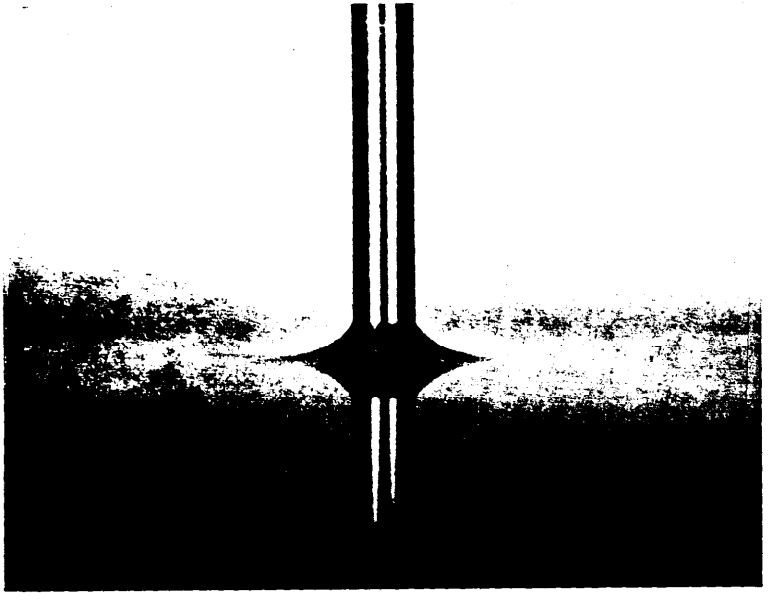

a

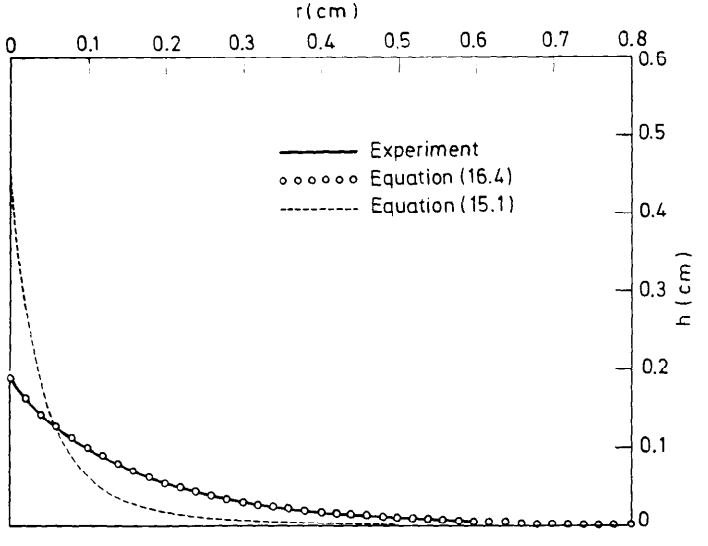

b

Fig. 4. a) The free surface on STP motor oil additive near a rod of radius $a=0.160$ cm rotating at $\omega=2.8$ rev/sec in a large vat; $\omega^4<144/a$, $\alpha=55°$.
b) Comparison of experimental and theoretical profiles ($\hat{\beta}=0.63$).

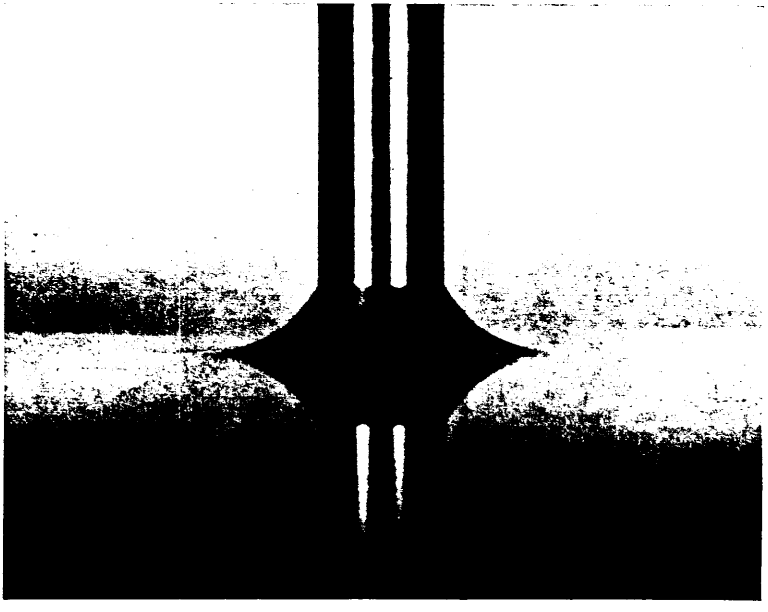

a

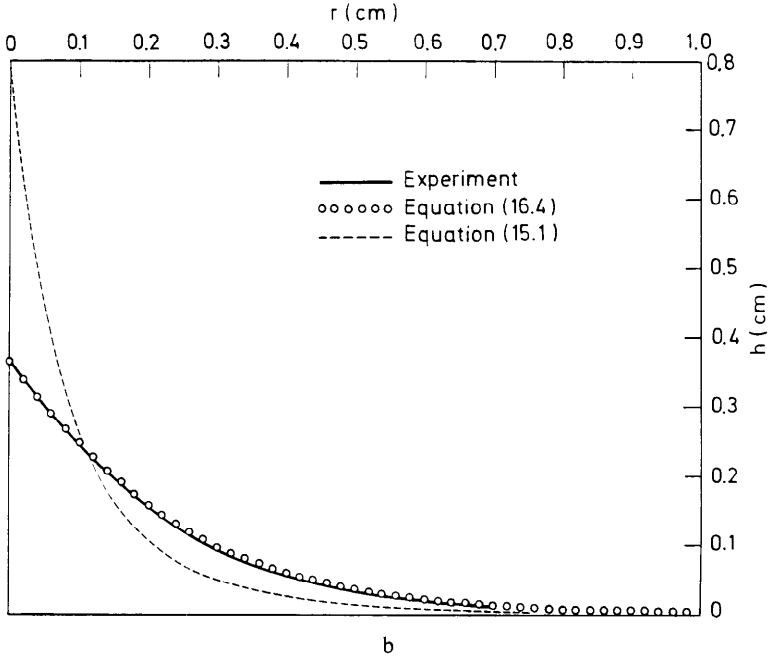

b

Fig. 5. a) The free surface on STP motor oil additive near a rod of radius $a=0.320$ cm rotating at $\omega=3.8$ rev/sec in a large vat; $\omega^4<144/a$, $\alpha=55°$.
b) Comparison of experimental and theoretical profiles ($\hat{\beta}=0.63$).

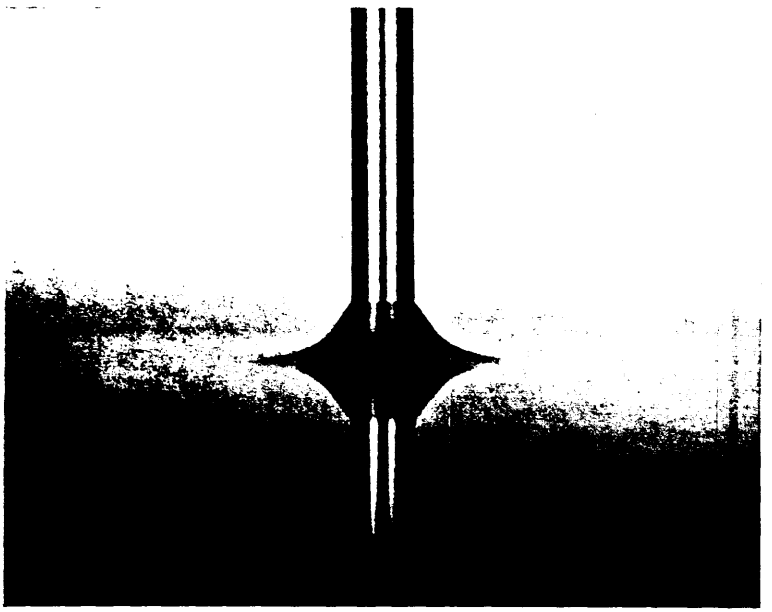

a

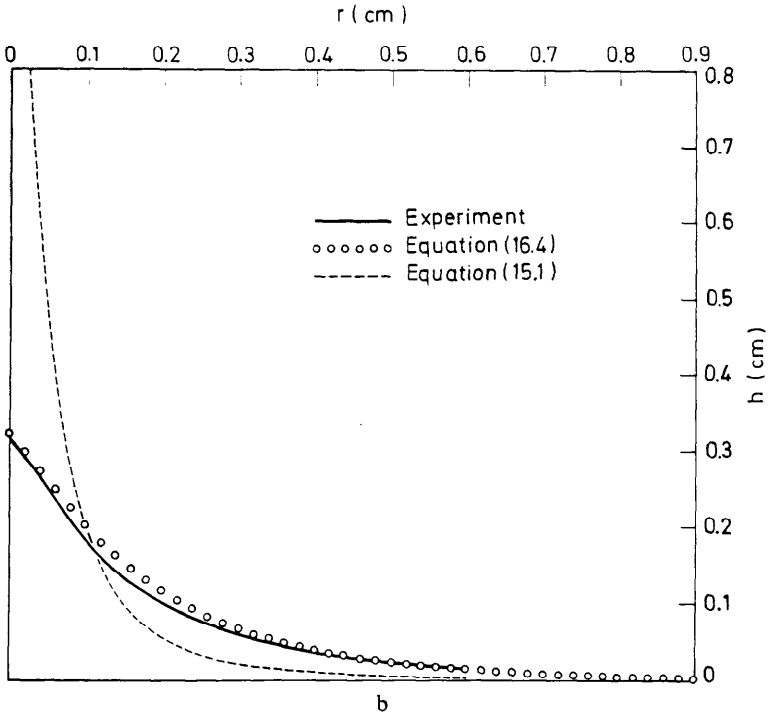

b

Fig. 6. a) The free surface on STP motor oil additive near a rod of radius $a=0.160$ cm rotating at $\omega=5.0$ rev/sec in a large vat; $\omega^4 < 144/a$, $\alpha=46°$.
b) Comparison of experimental and theoretical profiles ($\hat{\beta}=0.63$).

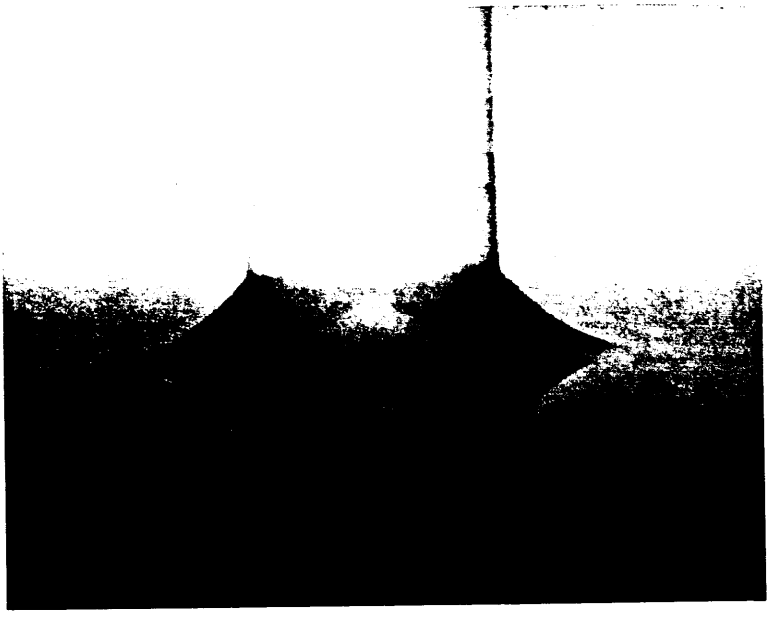

a

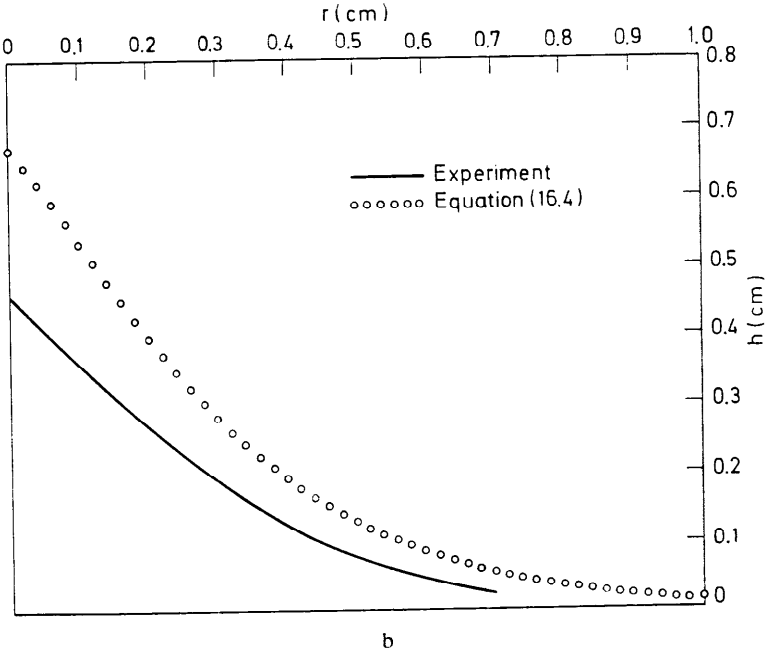

b

Fig. 7. a) The free surface on STP motor oil additive near a rod of radius $a=0.635$ cm rotating at $\omega=5.0$ rev/sec in a large vat; $\alpha=50°$.

b) Comparison of experimental profile with equation (16.4), $\hat{\beta}=0.63$. In this example $\omega^4>144/a$ and the effect of terms of higher order than second must be taken into account.

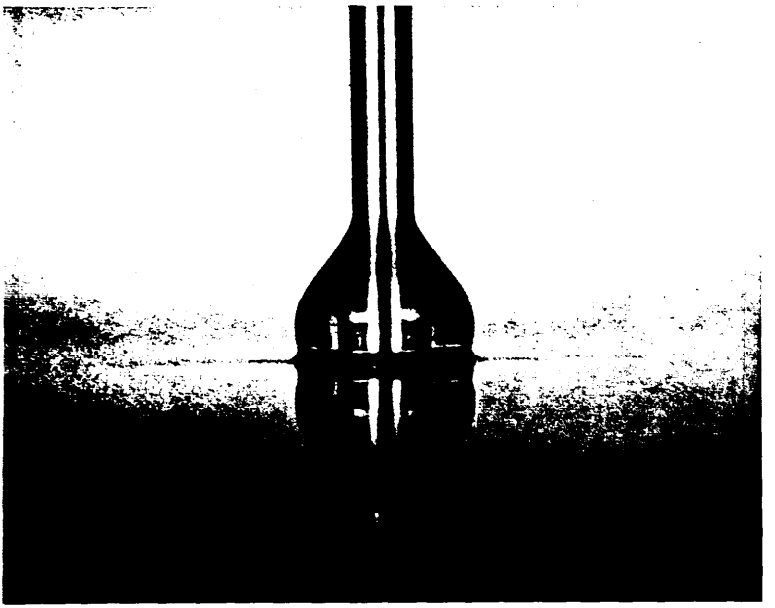

Fig. 8. The stable bubble of liquid formed near a rod of radius $a=0.160$ cm rotating at $\omega=$ 8.4 rev/sec ($\omega^4 > 144/a$) in a large vat of STP motor oil additive.

For larger values of ω^2 the rise at the rod increases less rapidly; the range of values of ω^2 for which $h(a; \omega^2, \varepsilon)$ varies linearly with ω^2 may, with fair accuracy, be given as $\omega^2 < 12/a^{\frac{1}{2}}$ (*cf.* footnote for (15.14)).

When $\omega^4 < 144/a$, the free surface of the liquid bubble has a concave shape, as shown in the photographs reproduced as Figs. 3(a) through 7(a), and in the profile graphs of Figs. 3(b) through 7(b). The experimental profile graphs in Figs. 3(b) through 7(b) were transposed from the photographs by projecting the photographic negative to 20 times actual size and carefully tracing the outline of the enlarged profile onto graph paper.

In the neighborhood of the value $\omega^4 = 144/a$, the free surface begins to assume a convex shape; this shape becomes increasingly more convex as ω is increased. Eventually the free surface around the rotating rod forms a drop-like shape which meets the main body of fluid at what appears to be a point of discontinuity of slope.* These drops appear to be very stable configurations. A typical example is shown in Fig. 8.

Finally, at even larger values of ω the steady drop-like configuration loses its stability to a motion periodic in time, which has a large effect on the instantaneous shape of the fluid surface. In the unsteady motion a band of fluid seems to rise slowly almost to the full height to which the fluid climbs up the rod and then to collapse downwards to the surface of the main body of fluid. Photographs taken at two different instants during a cycle are shown in Fig. 9. The periodic motion

* Close inspection of the apparent discontinuity revealed a smooth but very rapid variation of slope.

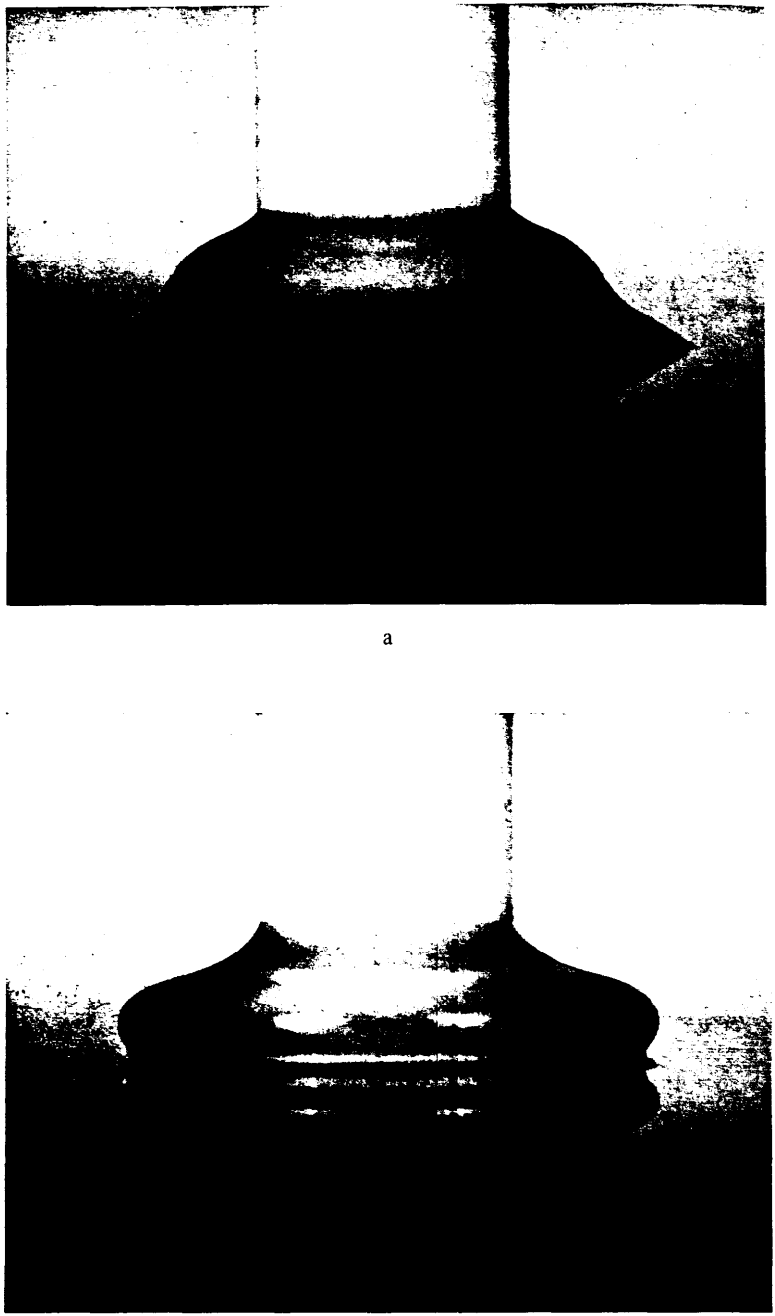

a

b

Fig. 9a and b. Two configurations assumed by the bubble of STP when the angular velocity (ω= 12.2 rev/sec) of the rod (a=0.635 cm) is such that the bubble is unstable to a motion periodic in time. The band of fluid shown near the top of the bubble in (a) collapses down to the surface of the fluid as shown in (b); it them climbs back to the position shown in (a).

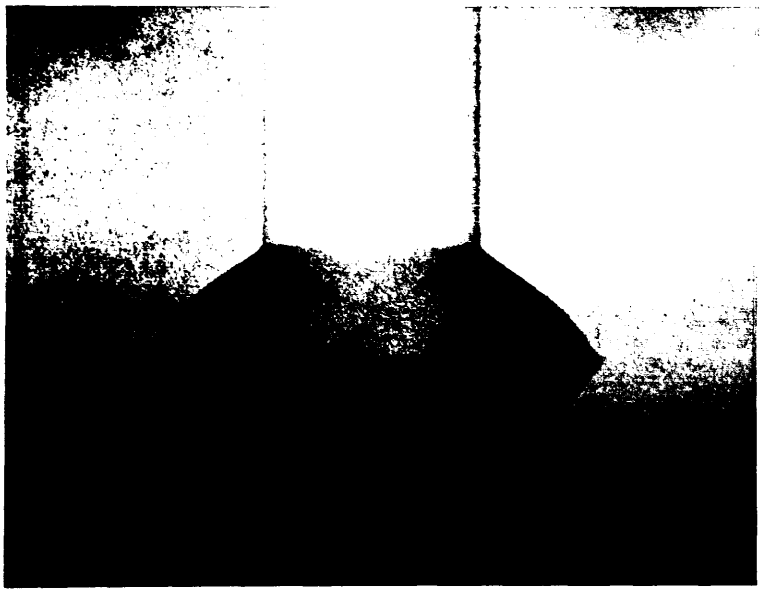

a

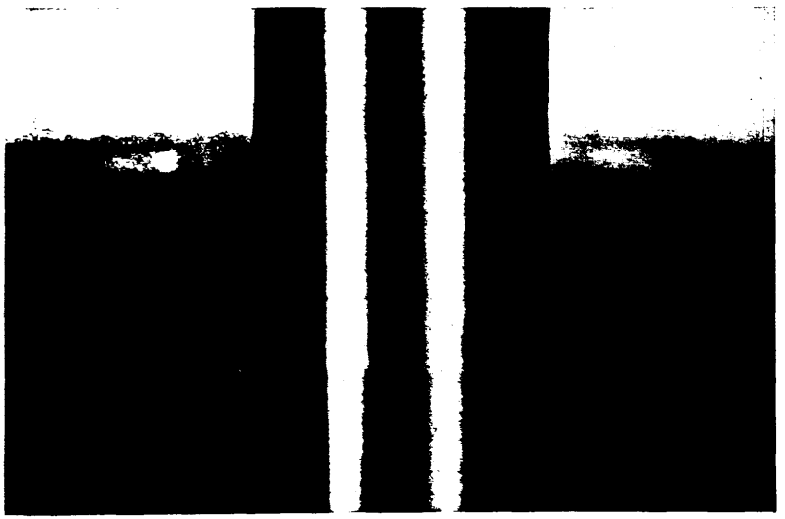

b

Fig. 10a and b. The effect of rod radius on the bubble shape for two different rods rotating at the same angular velocity in a large vat of STP, with $\omega^4 > 144/a$. a) $a = 0.635$ cm, $\omega = 10.0$ rev/sec; b) $a = 1.905$ cm, $\omega = 10.0$ rev/sec. The STP does not climb up the large rod, but instead it forms a depression similar to the one which would develop on the surface of a Newtonian fluid.

is very regular. However, if the angular velocity of the rod is increased further, the bubble configuration completely breaks down, and globules of fluid are thrown outwards from the bubble.

To correlate our observations with the predictions of analysis we need values for the following quantities:

(i) surface tension*, $T=30.9$ dynes/cm;
(ii) density of the fluid, $\rho=0.89$ gm/cm^3;
(iii) constitutive constants of second-order fluids*, $3\alpha_1+2\alpha_2\equiv\hat{\beta}$ (to be determined);
(iv) constitutive constants of higher-order fluids (to be considered in a later work); (16.1)
(v) radius a of the rod, in cm;

and

(vi) angular velocity, $\omega=\Omega/2\pi$ in rev/sec.

When all of these data are given, we can predict the rise and the shape of the free surface.

Fortunately, there is a sizable range of small values $\omega^4<144/a$ for which the higher-order corrections to (15.12) seem unimportant. In this range second-order effects are dominant. We wish to investigate the possibility that experimental observations of the rise lead to a reliable determination of the characterizing constant $\hat{\beta}$ of the second-order fluid. In addition we wish to compare theoretically predicted surface profiles with those obtained experimentally. The following procedure is used:

(a) For each rod the observed values of $h(a;\omega^2,\varepsilon)$ vary linearly with $\omega^2(\omega^4<144/a)$, as shown in Figs. 1 and 2. We identify the slope of this line as

$$\frac{dh_e}{d\omega^2}(a;0,\varepsilon). \tag{16.2}$$

(b) The theoretical values of (16.2) may be formed from (15.22). We find that

$$\frac{dh}{d\omega^2}=\frac{2\pi^2 a}{T\sqrt{S}}\left\{\frac{4\hat{\beta}}{4+\lambda}-\frac{\rho a^2}{2+\lambda}\right\}$$

where

$$(S)^{\frac{1}{2}}=5.32\ \text{cm}^{-1}\quad\text{and}\quad\lambda=a(S)^{\frac{1}{2}}.$$

Setting

$$\frac{dh_e}{d\omega^2}=\frac{dh}{d\omega^2}, \tag{16.3}$$

we may determine a value for the constitutive constant $\hat{\beta}$.

* We measured the surface tension of the STP motor oil additive over a range of temperatures encompassing room temperature with a standard ring tensiometer. The measured values vary only slightly with the temperature in the range near room temperature. More careful experiments are needed to determine the temperature dependence of the non-Newtonian coefficient $\hat{\beta}$.

Table 3. Determination of the values $\hat{\beta}$ by the method of (16.3). A single value $\hat{\beta}=0.63$ was obtained for rods of different diameter by fitting the surface profiles given by (16.4) to the observed profiles shown in Figs. 3–6. This method of best fitting and the method of (16.3) are independent; the rise of the profiles of Figs. 3–6 is not given in Figs. 1 and 2

	a (cm)	Type of Rod	$\hat{\beta}=3\alpha_1+2\alpha_2$ (gm/cm)
1.	0.945	Aluminum	0.94
2.	0.635	Aluminum	0.76
3.	0.635	Teflon	0.76
4.	0.635	Teflon	0.76
5.	0.320	Aluminum	0.63
6.	0.320	Teflon	0.63
7.	0.160	Aluminum	0.64
8.	0.160	Teflon	0.64

(c) Given $\hat{\beta}$, the functions

$$h^{[2,0]}(r; a, \hat{\beta})$$

are obtained by direct numerical integration of the boundary value problem (15.2 a, b, c).

Finally, theoretical surface profiles are computed from the equation

$$h(r; a, \omega^2, \hat{\beta}, \varepsilon)=h_s(r; a, \varepsilon)+2\pi^2\omega^2 h^{[2,0]}(r; a, \hat{\beta}) \tag{16.4}$$

where the values $h_s(r; a, \varepsilon)$ are computed numerically from the boundary-value problem (15.11 a, b, c).

The following points of agreement between theory and experiment merit emphasis:

(i) STP motor oil additive will climb up a small rod but not a large one. This fact follows most easily from equation (15.1), which neglects surface tension, but it follows also, with a more accurate estimate of the critical value of a, from setting $h(a; a, \omega, \hat{\beta}, \varepsilon)=0$ in (16.4). In the photographs reproduced Fig. 10 we have compared two rods of different diameters which rotate at the same speed; the effect of the rotation is to elevate the free surface at the smaller rod and to depress the free surface at the larger rod.

(ii) There is a realizable range of values ω for which the second order theory holds. This is demonstrated experimentally by the fact that h is proportional to the first power of ω^2 for a range of values of $\omega^4<144/a$, approximately.

(iii) The values of $\hat{\beta}$ computed from (16.3) are given in Table 3. The coefficient $\hat{\beta}$ should have a single value for all experiments on one and the same fluid at a given temperature. The value $\hat{\beta}\simeq 0.63$ was found repeatedly when small rods were

used, both for those listed in Table 3 and for the rods used in Figs. 3–7.* The increase of the value of $\hat{\beta}$ with rod diameter for the larger diameter rods is more than can be attributed to experimental error. This error may stem from temperature effects or from the terms of $O(\Omega^2)$ which are neglected in (15.12). (These neglected terms would necessarily vanish if we could make ε sufficiently small in the experiments.) The results given in Table 3 indicate that the rise is approximated by values computed from (16.4). From these results we may conclude that the rise increases linearly as the radius a of the rod, when a is small. On the other hand (15.1), which gives the rise when surface tension is neglected, implies that when a is small $dh/d\omega^2$ is independent of a. This possibility is in manifest disagreement with the experimental results, which show that $dh/d\omega^2$ increases very nearly linearly with a.

(iv) Rods of equal diameter but different materials (teflon and aluminum) have equal values of the slope $dh_e/d\omega^2$ (see (16.2)) but different values of the total height. The difference in the height can be explained by the fact that the tangent of the contact angle ($\tan\alpha = -\varepsilon$) was less for aluminum than for teflon. This equality of slope for differing radii and angular velocities but different values of ε suggest that $dh/d\omega^2$ is independent of ε for small values of ω^2 and a, as is assumed in the derivation of (15.14).

(v) The agreement between the observed surface profiles and the theoretical profiles calculated from (16.4) for $\omega^4 < 144/a$ is striking. The angular velocity of the rods shown in Figs. 3, 4, 5 and 6 satisfy the criterion $\omega^4 < 144/a$; the comparisons of theory with experiment in the figures is typical when $\omega^4 < 144/a$. On the other hand, for large values of ω and a, when $\omega^4 a > 144$, the profiles that occur in experiment differ from those predicted by (16.4). The rods shown

* A first independent determination of the value of $\hat{\beta}$ using the same STP motor oil additive was made in a Rheometrics Mechanical Spectrometer [1] using both cone and plate and parallel plate flows. The torque and normal thrust generated in these flows yield the shear stress S_{12} and the normal stress combinations $\sigma_2 - \sigma_1$ and σ_2 (see (2.11) and [2]). We are indebted to W. M. DAVIS & C. W. MACOSKO for making these measurements. They find that

$$\lim_{\kappa \to 0} \frac{\sigma_2 - \sigma_1}{\kappa^2} = -2\alpha_1 = 2.95 \pm 0.1 \text{ gm/cm}$$

and (16.5)

$$\lim_{\kappa \to 0} \frac{\sigma_2 - 2\sigma_1}{\kappa^2} = -(4\alpha_1 + \alpha_2) = 3.2 \pm 0.2 \text{ gm/cm}.$$

Thus

$$3\alpha_1 + 2\alpha_2 = \hat{\beta} = 0.98 \pm 0.5.$$

This value of $\hat{\beta}$ does not disagree with values in Table 3, which we have determined from our experiment on climbing.

A second independent determination of the value of $\hat{\beta}$ can be obtained using the values $-0.1 \geqq \sigma_1/(\sigma_2 - \sigma_1) \geqq -0.15$ which TANNER & KUO [3] and PIPKIN & TANNER [4] cite as representative for nearly all polyisobutylene solutions. Using this inequality and (16.5), we find that

$$0.6 \leqq 3\alpha_1 + 2\alpha_2 = \lim_{\kappa \to 0} \frac{2\sigma_1 + \frac{1}{2}(\sigma_2 - \sigma_1)}{\kappa^2} \leqq 0.9.$$

This inequality should be compared with the values given in Table 3.

in Figs. 6 and 7 both rotate at an angular velocity $\omega = 5.0$ rev/sec. However, in Fig. 6, $\omega^4 a = 625\ (0.160) < 144$, whereas in Fig. 7, $\omega^4 a = 625\ (0.635) > 144$.

All of the photographs shown in Figs. 3–7 were taken in a single experimental session, and a single value $\hat{\beta} = 0.63$ was used in the theoretical computations. The predicted profiles from equation (15.1), which neglects surface tension, shown as a faint dotted line in Figs. 3 through 6, are clearly not in good agreement with experiment.

Profiles were computed also for several of the experimental points shown in Figs. 1 and 2, with use of the values of $\hat{\beta}$ given in Table 3. The theoretical and experimental profiles were compared by use of the Polaroid slide method mentioned in the first paragraph of this section. The agreement between theory and experiment in these experiments was as good as the agreement exhibited in Figs. 3 through 6.

A comparison of our theory with experiments when ω is in the nonlinear range of the height curves of Figs. 1 and 2 cannot be made without prior computation of terms which appear at order higher than the second. It is possible that the range of agreement between theory and experiment can be considerably extended by including the leading terms of (15.13) in our analysis. It is already apparent, however, that the effect of the terms neglected is to inhibit the climbing which would be induced by the second-order terms alone.

This work was supported in part by the National Science Foundation.

References

1. Macosko, C.W., & J.M. Starita, SPE Tech. Papers **17**, 67 (1971) and SPE Journ. **27**, 38 (Nov. 1971).
2. Macosko, C.W., & W.M. Davis, "Flow between Eccentric Rotating Disks" presented at VI^e Congrès International de Rhéologie. Lyon, Sept. 1972.
3. Tanner, R.I., & Y. Kuo, "Some new measurements of the second normal stress", presented at VI^e Congrès International de Rhéologie. Lyon, Sept. 1972.
4. Pipkin, A.C., & R.I. Tanner, "A survey of theory and experiment in Viscometric Flows of Viscoelastic Liquids", Brown University Report.

Department of Aerospace Engineering
and Mechanics
University of Minnesota

(Received November 6, 1972)